Title
Valley splitting of Si/Si1−xGex heterostructures in tilted magnetic fields

Journal
Physical Review B, 73(16)

ISSN
2469-9950

Authors
Lai, K
Lu, TM
Pan, W
et al.

Publication Date
2006-04-15

DOI
10.1103/physrevb.73.161301

Peer reviewed

Valley splitting of $Si/Si_{1-x}Ge_x$ heterostructures in tilted magnetic fields

K. Lai,[1] T.M. Lu,[1] W. Pan,[2] D.C. Tsui,[1] S. Lyon,[1] J. Liu,[3] Y.H. Xie,[3] M. Mühlberger,[4] and F. Schäffler[4]

[1]*Department of Electrical Engineering, Princeton University, Princeton, New Jersey 08544*
[2]*Sandia National Laboratories, Albuquerque, NM 87185*
[3]*Department of Material Science and Engineering, UCLA, Los Angeles, CA 90095*
[4]*Institut für Halbleiterphysik, Universität Linz, A-4040 Linz, Austria*

(Dated: July 26, 2013)

We have investigated the valley splitting of two-dimensional electrons in high quality $Si/Si_{1-x}Ge_x$ heterostructures under tilted magnetic fields. For all the samples in our study, the valley splitting at filling factor $\nu = 3$ (Δ_3) is significantly different before and after the coincidence angle, at which energy levels cross at the Fermi level. On both sides of the coincidence, a linear density dependence of Δ_3 on the electron density was observed, while the slope of these two configurations differs by more than a factor of two. We argue that screening of the Coulomb interaction from the low-lying filled levels, which also explains the observed spin-dependent resistivity, is responsible for the large difference of Δ_3 before and after the coincidence.

PACS numbers: 73.43.Fg,73.21.-b

The study on the valley splitting of the two-dimensional electron gas (2DEG) confined in (001) Si surface has been highlighted by recent research effort on Si-based quantum computation[1]. For a Si 2DEG, only the two out-of-plane valleys are relevant since the other four in-plane valleys are lifted from the conduction band edge. To realize a functional Si quantum computer using spins as quantum bits, a large valley splitting that lifts the remaining two-fold degeneracy is desirable since the existence of two degenerate states associated with the $\pm k_z$ valleys is believed to be a potential source of spin decoherence [1]. In the single-particle picture, theories [2, 3, 4] in the early period of the 2D physics proposed that the surface electric field in the presence of 2D interface breaks the symmetry of these two valleys, resulting in an energy splitting proportional to the carrier density. The understanding of the valley splitting in real Si systems, however, is not a trivial task and requires much beyond such non-interacting band picture. In fact, the many-body effect [2, 4] was speculated to account for the enhancement over the bare valley splitting under strong magnetic (B) fields, while a detailed calculation is not yet available.

Experimental research on the valley splitting, on the other hand, was conducted mainly on the Si metal-oxide-semiconductor field-effect transistors (MOSFETs), in which the disorder effect is strong and direct measurement of the valley splitting proves to be difficult [5, 6]. More than a decade ago, the introduction of the graded buffer scheme significantly improved the sample quality of the Si/SiGe heterostructures [7]. To date, the valley splitting has been studied by various experimental techniques, including thermal activation [8], tilted field magnetotransport [9, 10], magnetocapacitance [11], microwave photoconductivity [12] and magnetization [13]. However, as pointed out by Wilde *et al.* in Ref. [13], results reported by different groups are ambiguous and inconsistent with previous band calculations. The nature of this valley splitting, especially its behavior under strong B-fields, stays as an unsettled problem.

Of the various methods used to study the valley splitting, tilted field magnetotransport, also known as the coincidence method [14], is frequently utilized. In a B-field tilted by an angle θ with respect to the 2D plane, the ratio of the cyclotron energy $E_C = \hbar\omega_C = \hbar eB_\perp/m^*$, where $B_\perp$ is the perpendicular field and m^* the effective mass, to the Zeeman energy $E_Z = g^*\mu_B B_{tot}$, where g^* is the effective g-factor, μ_B the Bohr magneton and B_{tot} the total field, can be continuously tuned by adjusting $\theta = \cos^{-1}(B_\perp/B_{tot})$. In particular, the so-called coincidence happens when the energy levels from different Landau levels (LLs) are aligned at the Fermi level. In a recent experiment [15], the inter-valley energy gaps at the odd-integer quantum Hall (QH) states were studied and found to rise rapidly towards the coincidence. In this work, we show that the anomalous rise was not observed in the even-integer QH states, whose energy gaps close as θ approaches the single-particle degenerate points. For all the samples in our study, the $\nu = 3$ valley splitting before the coincidence follows a linear density dependence that extrapolates to about -0.4K at zero density, which is probably due to level broadening. The $\nu = 3$ gap after the coincidence also depends linearly on density, while the slope increases by more than a factor of two. We argue that screening of the Coulomb interaction from the low-lying filled levels, which also explains the observed spin-dependent resistivity, is responsible for the change of the observed $\nu = 3$ gaps on different sides of the coincidence.

The specimens in our study are modulation-doped n-type Si/SiGe heterostructures grown by molecular-beam epitaxy. Important sample parameters, such as the electron density (n), mobility (μ) and width of the quantum well (W), are listed in Table. 1. For the

samples labeled as LJxxx, relaxed $Si_{0.8}Ge_{0.2}$ buffers provided by Advanced Micro Devices (AMD) were used as substrates, followed by a 1 μm $Si_{0.8}Ge_{0.2}$ buffer layer prior to the growth of the strained Si channel. On top of the Si quantum well, a 20nm $Si_{0.8}Ge_{0.2}$ spacer, a delta-doped Sb layer, a 25nm $Si_{0.8}Ge_{0.2}$ cap, and a 4nm Si cap layer are subsequently grown. The carrier density is controlled by the amount of Sb dopants. The high mobility sample labeled as 1317 is the same specimen as that used in Ref. [15] and its density and mobility can be tuned by controlling the dose of low temperature illumination by a light-emitting diode (LED).

Sample	$n(10^{11}\mathrm{cm}^{-2})$	$\mu(\mathrm{m}^2/\mathrm{Vs})$	W(nm)	Illumination
LJ122	3.1	6.3	10	No
LJ126	2.3	9.8	10	Saturated
LJ127	2.1	8.7	10	Saturated
LJ139	1.7	12	20	Saturated
1317-I	1.4	19	15	No
1317-II	1.8	22	15	Unsaturated
1317-III	2.4	25	15	Saturated

Table 1. List of sample parameters. The density, mobility and width of the quantum well are shown, together with the dose of illumination.

Magnetotransport measurements were performed in the 18/20T superconducting magnet in the National High Magnetic Field Laboratory (NHMFL) in Tallahassee, FL. Samples were sitting in a rotating stage at the dilution refrigerator with a base temperature T_{base} = 20mK. Standard low frequency (5∼13Hz) lock-in techniques were used to measure the diagonal resistivity ρ_{xx} and the Hall resistivity ρ_{xy}.

In Fig. 1, we show the ρ_{xx} traces as a function of the filling factor (ν) at several tilt angles for samples (a) 1317-I and (b) 1317-III. The odd-integer QH states ν = 3, 5... are associated with energy gaps opened by the valley splitting. The three tilt angles were chosen so that from the bottom to the top traces, $1/\cos\theta$ = 1 (before the 1st coincidence), ∼ 3.7 (between the 1st and 2nd coincidences) and ∼ 5.6 (after the 2nd coincidence), respectively. We will return to the tilt-field data later in the discussion.

Fig. 2a shows a schematic of the tilted-field energy diagram of a Si 2DEG. The LL (N), spin (↑ or ↓) and valley (+ or −) indices are indicated in the plot. Since Δ_v is shown to be independent of the parallel field [8, 15], the two valley states originated from each spin level are parallel to each other in the diagram. In this independent-electron picture, the levels are not affected as they cross each other, and the energy gap of individual QH states closes at certain tilt angles, or coincidence angles. Since in a Si 2DEG, Δ_v is usually much smaller than E_Z and

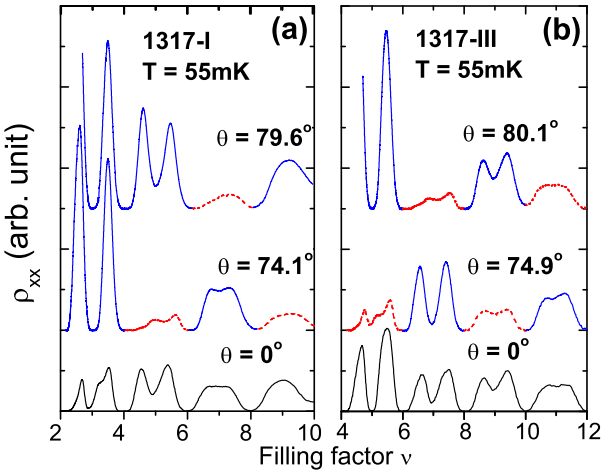

FIG. 1: Magnetoresistivity ρ_{xx} as a function of the filling factor for samples (a) 1317-I and (b) 1317-III at selected tilt angles at T = 55mK. From bottom to top, the system is before the 1st coincidence ($\theta = 0^o$), between the 1st and 2nd coincidences ($\theta \sim 74^o$), and after the 2nd coincidence ($\theta \sim 80^o$). After the 1st coincidence, the overall amplitude of the ρ_{xx} is generally higher when electrons in the Fermi level have up-spins (solid blue curves) and lower for down-spins (dashed red curves).

E_C, we adopt the conventional notation that the jth order coincidence occurs when E_Z / E_C roughly equals an integer number j. In Fig. 2b and 2c, the energy gaps, obtained by fitting $\rho_{xx} \propto \exp(-\Delta_3/2k_BT)$ in the thermal activation regime, at ν = 4 and 6 in sample 1317-I are shown as a function of $1/\cos\theta$ or $B_{tot}/B_\perp$. When θ is away from the coincidences, the gaps at ν = 4 and 6 vary linearly with respect to $1/\cos\theta$ with a slope corresponding to g^* = 2, consistent with the independent-electron model. On the other hand, the even-integer energy gaps drop suddenly towards the coincidence angles at which the single-particle gap closes, e.g., $1/\cos\theta \sim 2.5$ (1st coincidence) for ν = 4 and $1/\cos\theta \sim 4.5$ (2nd coincidence) for ν = 6, as can be seen in Fig. 2b and 2c. This sudden drop of activation gap towards the degenerate points was observed in a wide GaAs/AlGaAs quantum well and explained within the framework of quantum Hall ferromagnetism [16].

In contrast to the well-behaved even-integer QH states, the energy gap of the ν = 3 state (Δ_3) exhibits an anomalous rise towards the coincidence, as shown in the inset of Fig. 3, a phenomenon previously reported in Ref. [15]. We emphasize here that such an anomaly was observed in all the samples investigated in this study, in spite of the considerable difference in the sample structure and mobility. Out of the coincidence region, the activation energy is indeed independent of the parallel field component, while it differs by about a factor of 3 (0.8K vs. 2.1K) on different sides of the coincidence. Referring to

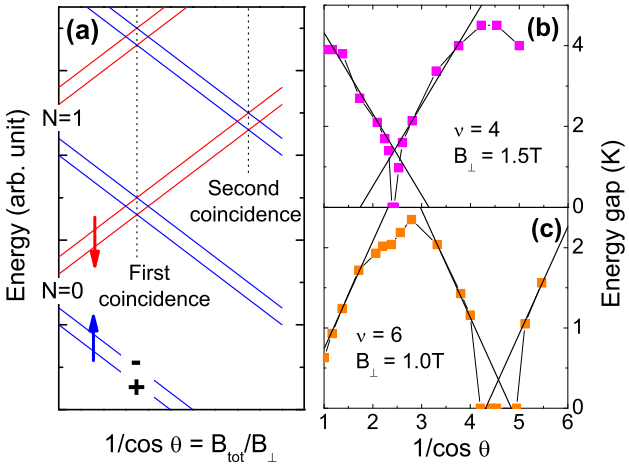

FIG. 2: (a) Schematic of the LL fan diagram in tilted B-fields. The LL (N), spin (↑ or↓) and valley (+ or −) indices are indicated for each level. The positions of the 1st and 2nd coincidences are indicated. (b) Measured energy gaps at $\nu = 4$ ($B_\perp = 1.5$T) and (c) $\nu = 6$ ($B_\perp = 1.0$T) of sample 1317-I as a function of $1/\cos\theta$ or $B_{tot}/B_\perp$. The solid lines correspond to $g^* = 2$.

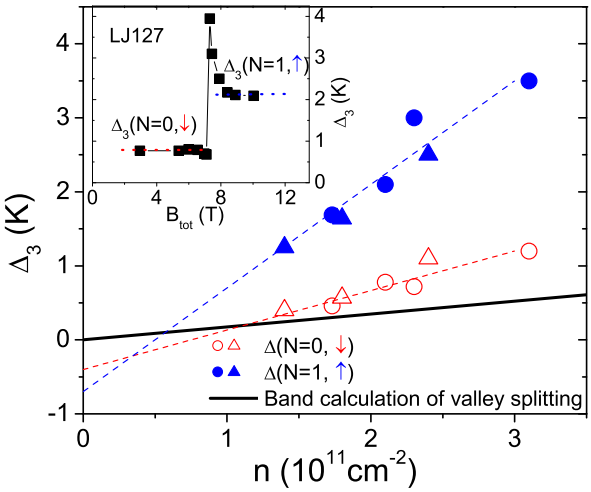

FIG. 3: Density dependence of the valley splitting at $\nu = 3$. The empty symbols (triangles for samples 1317 and circles for LJxxx) stand for Δ_3(N=0,↓) and the filled symbols for Δ_3(N=1,↑). Dashed lines are linear fits to the data and extrapolate to finite values at zero density. The solid line shows the band calculation of valley splitting in Ref. [2]. The inset shows the Δ_3 gap of sample LJ127 as a function of B_{tot}. The coincidence occurs around $B_{tot} = 7$T.

the level diagram in Fig. 2a, we label the valley splitting as Δ_3(N=0,↓) and Δ_3(N=1,↑) before and after the coincidence, respectively.

In Fig. 3, we plot the measured Δ_3(N=0,↓) and Δ_3(N=1,↑) gaps for all 7 samples as a function of the carrier density. The band calculation of valley splitting in a Si 2DEG [2, 3, 4] based on the effective-mass approximation, showing a linear dependence Δ_v (K) $\sim 0.17n$ (10^{11}cm^{-2}) at B = 0, is also plotted (solid line) for comparison. Despite some scattering in the data, the measured Δ_3(N=0,↓) gaps essentially fall on a straight line that extrapolates to -0.4±0.2K at zero density. We note that this energy of -0.4K is within the order of the sample-dependent disorder broadening ($\Gamma \sim \hbar/\tau = \hbar e/m^*\mu$, where τ is the transport scattering time), which lies between 0.3K and 1.1K in our samples. Interestingly, the detailed sample structure, e.g., the well width W, seems less important here. The Δ_3(N=1,↑) gaps of the same set of samples also fall onto a line extrapolating to -0.7±0.3K at $n = 0$, again within the order of level broadening. On the other hand, the slope of the linear density dependence differs by more than a factor of 2 (0.5K vs. 1.4K per 10^{11}cm^{-2}) before and after the coincidence. And both are significantly higher than that of the band calculation at B=0.

The linear density dependence of the valley gaps and strong enhancement over the bare valley splitting were recently reported in a Si-MOSFET system using magnetocapacitance method [11]. The authors pointed out that the electron-electron (e-e) interaction, especially the exchange interaction, is likely to account for the observed large valley gaps. In order to shed some light to the apparent large difference between the Δ_3(N=0,↓) and Δ_3(N=1,↑) gaps, we scrutinize the many-body effect for the two configurations of $\nu = 3$, shown in Fig. 4. For the relevant perpendicular B-fields in this work, the e-e interaction energy $E_{e-e} \sim e^2/4\pi\epsilon l_B$ ($l_B = (\hbar/eB_\perp)^{-1/2}$ is the magnetic length) is larger than the LL spacing so mixing between different LLs has to be taken into account. Consequently, we explicitly include the lower two filled levels (N=0, ↑, ±), which are kept intact for all tilt angles, into the analysis. Before the coincidence, electrons in these two low-lying levels have the same LL but opposite spin indices comparing to the ones near the Fermi level (E_F). Since the Pauli exclusion principle does not prevent the opposite spins from approaching each other, these low-lying electrons can come close to the electrons at E_F and strongly screen the Coulomb interaction. The enhancement of the $\nu = 3$ gap due to the electron-electron interaction is thus much reduced and the gap is close to the bare value at this LL. On the other side of the coincidence, however, such screening is much less effective. First, the electrons near E_F are from the N=1 LL and their wave function is different from the N=0 levels. The off-diagonal matrix element of this Coulomb energy between the two different LLs should be considerably smaller than that from the same LL. Second, even in the presence of LL mixing effect, the exclusion principle limits the screening between the same up-spin levels. As a result, the Δ_3(N=1,↑) gap is greatly enhanced over the bare valley splitting. We nevertheless emphasize here that in the last few LLs, the shape of the wave function

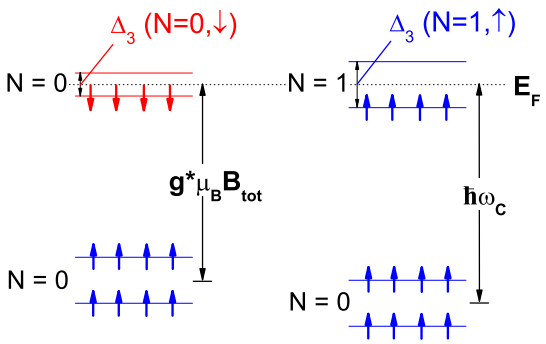

FIG. 4: Level diagram at $\nu = 3$ before (left) and after (right) the coincidence. E_F resides in the gap between the lowest empty levels and the top filled levels. The level occupation, as well as the spin orientation, is indicated in the plot. Before the coincidence, the low-lying (N=0,↑,±) electrons, separated by $E_Z = g^*\mu_B B_{tot}$ from the Fermi level, strongly screen the Coulomb interaction for electrons near E_F, resulting in a less enhanced Δ_3(N=0,↓) over the bare valley splitting. The same screening, on the other hand, is less effective from the like-spin charges in a different LL, giving a large Δ_3(N=1,↑).

is completely different from the plane wave at B = 0. So even the bare valley splitting here could be different from the results obtained by Ohkawa and Uemura [2], who only consider high LLs by using simple average over the in-plane k-vector.

Finally, we note that the spin-dependent resistivity, first reported by Vakili *et al.* [17] and successfully explained by screening from the filled LLs, is also observed in our samples. In Fig. 1, after the 1st coincidence, the overall ρ_{xx} amplitude is lower (dashed red curves) when the spins at the Fermi level orient opposite to the majority up-spins in the system and higher when the two are aligned (solid blue curves), which was attributed to screening from the low-lying filled LLs. Due to the exclusion principle, electrons with same spins cannot approach each other to effectively screen the disorder potential, resulting in a higher ρ_{xx} comparing to the opposite case. Interestingly, the same alternating pattern is also observed in the strengths of the odd-integer valley states.

In summary, we have carried out a titled field study of the Si/SiGe heterostructures and measured the energy gaps of integer QH states as a function of the tilt angle. The gaps at the even-integer fillings follow qualitatively the independent-electron picture, while the odd-integer states show rapid rise towards the coincidence angles. For all the samples we studied, the $\nu = 3$ valley splitting on both sides of the coincidence shows linear density dependence with significantly different slopes. The difference of the Δ_3(N=0,↓) and Δ_3(N=1,↑) gaps, as well as the observed spin-dependent resistivity, can be qualitatively explained by screening of the Coulomb interaction from the low-lying filled levels.

This work is supported by the NSF, the DOE and the AFOSR and the AFOSR contract number is FA9550-04-1-0370. We thank Dr. Qi Xiang of AMD for supplying us with the high quality relaxed SiGe substrates. Sandia National Labs is operated by Sandia Corporation, a Lockheed Martin Company, for the DOE. The experiment performed in NHMFL is under the project number 3007-081. We thank E. Palm, T. Murphy, G. Jones, S. Hannahs and B. Brandt for their assistances and Y. Chen and D. Novikov for illuminating discussions.

[1] M. Xiao, I. Martin, E. Yablonovitch, and H.W. Jiang, Nature (London) **430**, 435 (2004) and references therein.
[2] F.J. Ohkawa and Y. Uemura, J. Phys. Soc. Jpn. **43**, 917 (1977).
[3] L.J. Sham and M. Nakayama, Phys. Rev. B **20**, 734 (1979).
[4] T. Ando, A.B. Fowler, and F. Stern, Rev. Mod. Phys. **54**, 437 (1982).
[5] R. J. Nicholas, K. von Klitzing and T. Englert,, Solid State Commun. **34**, 51 (1980).
[6] V. M. Pudalov, S. G. Semenchinski, and V. S. Edel'man, JETP Lett. **41**, 325 (1985).
[7] F. Schäffler, Semicond. Sci. Technol. **12**, 1515 (1997) and references therein.
[8] P. Weitz, R.J. Haug, K. von Klitzing and F. Schäffler, Surf. Sci. **361/362**, 542 (1996).
[9] S.J. Koester, K. Ismail and J.O. Chu, Semicond. Sci. Tech. **12**, 384 (1997).
[10] H.W. Schumacher, A. Nauen, U. Zeitler, R.J. Haug, P. Weitz, A.G.M. Jansen and F. Schäffler, Physica B **256-258**, 260 (1998).
[11] V.S. Khrapai, A.A. Shashkin and V.T. Dolgopolov, Phys. Rev. B **67**, 113305 (2003).
[12] S. Goswami, J.L. Truitt, C. Tahan, L.J. Klein, K.A. Slinker, D.W. van der Weide, S.N. Coppersmith, R. Joynt, R.H. Blick, M.A. Eriksson, J.O. Chu and P. M. Mooney, cond-mat/0408389.
[13] M. A. Wilde, M. Rhode, C. Heyn, D. Heitmann, D. Grundler, U. Zeitler, F. Schäffler, R. J. Haug, Phys. Rev. B **72**, 165429 (2005).
[14] F.F. Fang and P.J. Stiles, Phys. Rev. **174**, 823 (1968).
[15] K. Lai, W. Pan, D.C. Tsui, S. Lyon, M. Mühlberger and F. Schäffler, cond-mat/0510599.
[16] K. Muraki, T. Saku, and Y. Hirayama, Phys. Rev. Lett. **87**, 196801 (2001).
[17] K. Vakili, Y. P. Shkolnikov, E. Tutuc, N. C. Bishop, E. P. De Poortere, and M. Shayegan, Phys. Rev. Lett. **94**, 176402 (2005).